2010 International Conference on Mechanical and Electrical Technology (ICMET 2010)

Speed Control of PMBLDC Motor Using MATLAB/Simulink and Effects of Load and Inertia Changes

V M Varatharaju
Research Scholar, Department of EEE,
Anna University, Chennai, INDIA,600 025,
(vmvraj@gmail.com).

B L Mathur
Professor, Department of EEE
SSN College of Engineering, Kalavakkam,
INDIA,603 110, (blmathur@ssn.edu.in)

K Udhyakumar
Assistant Professor, Department of EEE,
Anna University, Chennai, INDIA, 600 025,
(k_udhayakumar@annauniv.edu).

Abstract: **Modeling and simulation of electromechanical systems with machine drives are essential steps at the design stage of such systems. This paper describes the procedure of deriving a model for the brushless dc motor with 120-degree inverter system and its validation in the MATLAB/Simulink platform. The discussion arrives at a closed-loop speed control, in which PI algorithm is adopted and the position-pulse determination is done through current control for a standard trapezoidal BLDC motors. The simulation results for BLDC motor drive systems confirm the validity of the proposed method.**

Keywords: PMBLDC Motor, simulation and modeling, speed control.

I. INTRODUCTION

Recently, permanent magnet brushless dc motors (PMBLDCM) are widely used in many applications such as motors, sensors, actuators, etc [1]. Permanent magnet motors with trapezoidal back EMF and sinusoidal back EMF have several advantages over other motor types. Most notably, (compared to dc motors) they are lower maintenance due to the elimination of the mechanical commutator and they have a high-power density which makes them ideal for high-torque-to weight ratio applications [2]. Compared to induction machines, they have lower inertia allowing for faster dynamic response to reference commands. Also, they are more efficient due to the permanent magnets which results in virtually zero rotor losses [3]. Permanent magnet brushless dc (PMBLDC) motors could become serious competitors to the induction motor for servo applications. The PMBLDC motor is becoming popular in various applications because of its high efficiency, high power factor, high torque, simple control and lower maintenance [4]. The major disadvantage with permanent magnet motors is their higher cost and relatively higher complexity introduced by the power electronic converter used to drive them. The added complexity is evident in the development of a torque/speed regulator [5]. The magnetization directions and intensities are analyzed using finite element analysis with a detailed magnetization procedure for ferrite bonded magnets used in inner-rotor type BLDC motors [6]. The effect of stator resistance on average-value modeling of electromechanical systems consisting of BLDC motor and 120-degree inverter systems, including commutation current has been presented [7]. It is shown that the model becomes more accurate both in time and frequency domains for the motors with large stator resistance (small electrical time constant of the stator winding) typically operate with small commutation angle. *Bhim singh, B P singh and K Jain* have proposed a digital speed controller for BLDCM and implemented in a digital signal processor [8]. Later in 1998 *peter vas* has developed scheme to extract the rotor position and the speed of BLDC motor by Extended Kalman Filter (EKF) [9]. *M.Jadric and B.Terzic* have successfully adapted the Hall Effect sensor to sense the rotor position for every 60 degree electrical [10].

Due to the extensive use of modeling and simulation and the heavy reliance on their accuracy, both simulation speed and model accuracy are very important. For the purposes of stability analysis and controller design, it is often desirable to investigate the large-signal transients and small-signal characteristics of the system. Simulation studies are also often performed many times to achieve the required design goals. In this study, the nonlinear simulation model of the BLDC motors drive system with proportional-integral (PI) control based on MATLAB/Simulink platform is presented. The simulated results in terms of electromagnetic torque and rotor speed are given.

II. NARRATIVE OF PMBLDCM DRIVE

Fig.1 shows the typical BLDC motor controlled by an inverter. Typical Hall-sensor-controlled BLDC motors, such as the one considered in this paper, is very common. The inverter converts a dc source voltage into 3-phase ac voltages with frequency corresponding to the rotor position and speed. This paper focuses on typical Hall-sensor controlled VSI-driven BLDC motors, where the inverter operates using 120-degree commutation method. Rotor position is sensed by Hall Effect sensors embedded into the stator which gives the

978-1-4244-8102-6/10/$26.00 © 2010 IEEE

sequence of phases. Whenever the rotor magnetic poles pass near the Hall sensors, they give a high/low signal, indicating the N or S pole is passing near the sensors. The three Hall sensors, *H*1, *H*2, and *H*3, are used to detect the rotor position. To rotate the BLDC motor, the stator windings should be energized in a sequence. Based on the combination of these three Hall sensor signals, the exact sequence of commutation can be determined

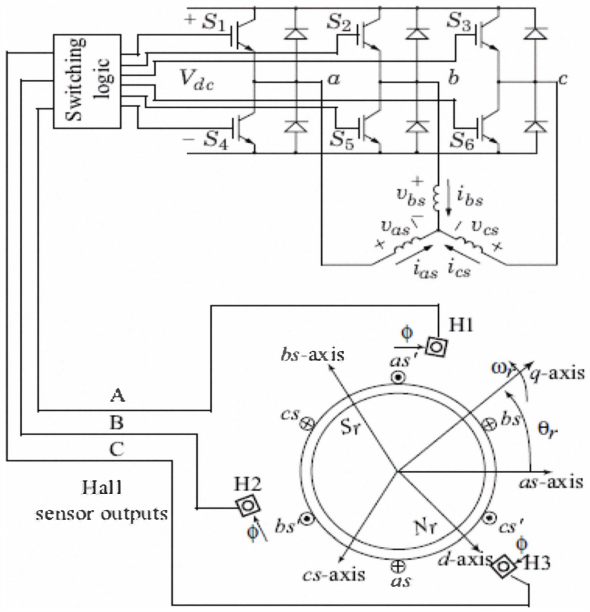

Figure 1. BLDC Motor controlled by the inverter

A. *Closed Loop Control*

Fig.2 describes the basic building blocks of the PMBLDCM drive system. The drive consists of speed controller, reference current generator, pulse width modulation (PWM) current controller, position sensor, the motor and a IGBT based voltage source inverter (CC-VSI). The speed of the motor is compared with its reference value and the speed error is processed in PI speed controller. The output of this controller is considered as the reference torque. A limit is put on the speed controller output depending on permissible maximum winding currents. The reference current generator block generates the three phase reference currents (i_a*, i_b*, ic*) using the limited peak current magnitude decided by the controller and the position sensor. The PWM current controller regulates the winding currents (i_a, i_b, i_c) within the small band around the reference currents(i_a*, i_b*, i_c*). The motor currents are compared with the reference currents and the switching commands are generated to drive the power switches.

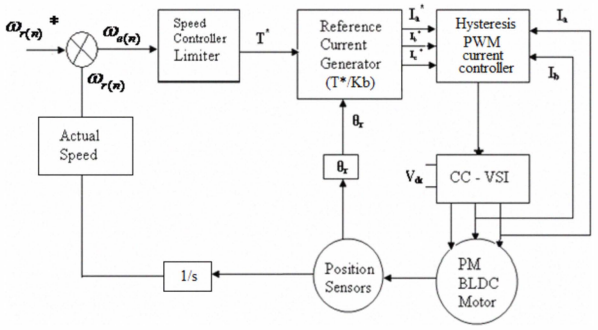

Figure 2. PMBLDC motor drive system

The PI controller is widely used in industry due to its ease in design and simple structure. The rotor speed $\omega_r(n)$ is compared with the reference speed $\omega_r(n)$* and the resulting error is estimated at the n^{th} sampling instant as:

$$\omega_e(n) = \omega_r(n)^* - \omega_r(n) \quad (1)$$

The new value of torque reference is given by

$$T(n) = T(n-1) + K_P\omega_e(n) - \omega_e(n-1) + K_1\omega_e(n) \quad (2)$$

Where, 'ω_e(n−1)' is the speed error of previous interval, and 'ω_e(n)' is the speed error of the working interval. K_P and K_I are the gains of proportional and integral controllers respectively. By using Ziegler Nichols method the K_P and K_I values are determined [11].

B. *Reference Current Generator*

The magnitude of the reference current (I*) is determined by using reference torque (T*) and the back emf constant (K_b); $I^* = \frac{T^*}{K_b}$ [12]. Depending on the rotor position, the reference current generator block generates three-phase reference currents (i_a*, i_b*, i_c*) considering the value of reference current magnitude as I*, − I* and zero. The reference current generation is explained in the Table.1.

Table 1.Rotor position signal Vs reference current

Rotor Position Signal θ_r	**Reference Currents** (i_a*, i_b*, i_c*)		
θ° - 60°	I*	−I*	0
60° - 120°	I*	0	−I*
120° -180°	0	I*	−I*
180° - 240°	−I*	I*	0
240° - 300°	−I*	0	I*
300° - 360°	0	−I*	I*

C. PWM Current Controller

The PWM current controller contributes to the generation of the switching signals for the inverter switches. The switching logic is formulated as given below.

If $i_a < (i_a^*)$ switch 1 ON and switch 4 OFF
If $i_a > (i_a^*)$ switch 1 OFF and switch 4 ON
If $i_b < (i_b^*)$ switch 3 ON and switch 6 OFF
If $i_b > (i_b^*)$ switch 3 OFF and switch 6 ON
If $i_c < (i_c^*)$ switch 5 ON and switch 2 OFF
If $i_c > (i_c^*)$ switch 5 OFF and switch 2 ON

III. MODELING

A. Back EMF

The phase back emf in the PMBLDC motor is trapezoidal in nature and also a function of the speed (ω_r) and rotor position angle (θ_r) as shown in Fig.3.

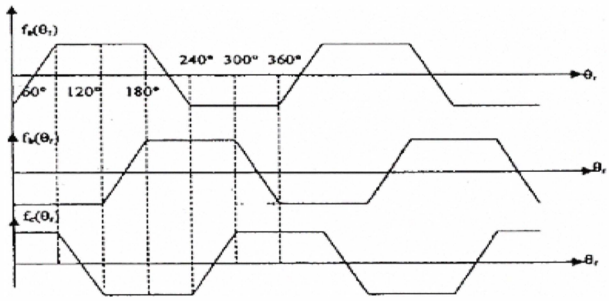

Figure 3. Components of back EMF

The normalized function of back emfs is shown in Fig.5. From this, the phase back emf e_{an} can be expressed as

$$\begin{aligned} f_a(\theta_r) &= E && 0^0 < \theta_r < 120^0 \\ f_a(\theta_r) &= (6E/\pi)(\pi - \theta_r r) - E && 120^0 < \theta_r < 180^0 \\ f_a(\theta_r) &= -E && 180^0 < \theta_r < 300^0 \\ f_a(\theta_r) &= (6E/\pi)(\theta_r r - 2\pi) + E && 300^0 < \theta_r < 360^0 \end{aligned} \quad (3)$$

Where, $E=K_b\omega_r$ and e_{an} can be described by E and normalized back emf function $f_a(\theta_r)$ $[e_{an} = E\, f_a(\theta_r)]$.

The back emf functions of other two phases (e_{bn} and e_{cn}) can also be determined in similar way using E and the normalized back emf function $f_b(\theta_r)$ and $f_c(\theta_r)$.

IV. PMBLDC MOTOR AND INVERTER

The PMBLDC motor is modeled in the 3-phase abc frame. The general volt-ampere equation for the circuit shown in the Fig.4 can be expressed as:

$$V_{an} = Ri_a + p\lambda_a + e_{an} \quad (4)$$
$$V_{bn} = Ri_b + p\lambda_b + e_{bn} \quad (5)$$
$$V_{cn} = Ri_c + p\lambda_c + e_{cn} \quad (6)$$

Where, V_{an}, V_{bn} and V_{cn} are phase voltages and may be defined as:

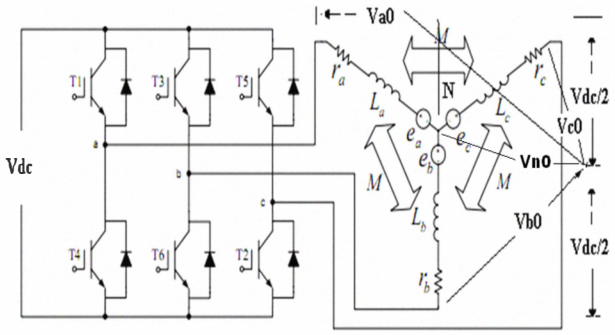

Figure 4. Inverter circuit with PMBLDCM drive

$$\begin{aligned} V_{an} &= V_{a0} - V_{n0}, \\ V_{bn} &= V_{b0} - V_{n0}, and \\ V_{c0} &= V_{c0} - V_{n0}. \end{aligned} \quad (7)$$

Where V_{a0}, V_{b0}, V_{c0} and V_{n0} are three phase and neutral voltages with respect to the zero reference potential at the mid-point of dc link (0) shown in the Fig.4. R is the resistance per phase of the stator winding, p is the time differential operator, and e_{an}, e_{bn} and e_{cn} are phase to neutral back emfs. The λ_a, λ_b and λ_c are total flux linkage of phase windings a, b and c respectively. Their values can be expressed as:

$$\lambda_a = L_S i_a - M(i_b + i_c) \quad (8)$$
$$\lambda_b = L_S i_b - M(i_a + i_c) \quad (9)$$
$$\lambda_c = L_S i_c - M(i_a + i_b) \quad (10)$$

Where, 'L_s' and 'M' are self and mutual inductances respectively.

The PMBLDC motor has no neutral connection and hence this results in,

$$i_a + i_b + i_c = 0 \quad (11)$$

Substituting (11) in (8), (9) and (10), the flux linkages are obtained.

$$\begin{aligned} \lambda_a &= i_a(L_S + M), \\ \lambda_b &= i_b(L_S + M), and \\ \lambda_c &= i_c(L_S + M) \end{aligned} \quad (12)$$

By substituting (12) in volt-ampere relations (4)-(6) and rearranging these equations in a current derivative of statespace form, gives,

$$pi_a = 1/(L_S + M)(V_{an} - Ri_a - e_{an}) \quad (13)$$
$$pi_b = 1/(L_S + M)(V_{bn} - Ri_b - e_{bn}) \quad (14)$$

$$pi_c = 1/(L_S + M)(V_{cn} - Ri_c - e_{cn}) \quad (15)$$

The developed electromagnetic torque may be expressed as

$$T_e = (e_{an}i_a + e_{bn}i_b + e_{cn}i_c)/\omega_r \quad (16)$$

Where, 'ω_r' is the rotor speed in electrical rad/sec. Substituting the back emfs in normalized form, the developed torque is given by

$$T_e = K\{f_a(\theta_r)i_a + f_b(\theta_r)i_b + f_c(\theta_r)i_c\} \quad (17)$$

The mechanical equation of motion in speed derivative form can be expressed as:

$$p\omega_r = (P/2)(T_e - T_L - B\omega_r)/J \quad (18)$$

Where, 'P' is the number of poles, 'T_L' is the load torque in N-m, 'B' is the frictional coefficient in Nm/rad, and 'J' is the moment of inertia in kg-m^2.

The derivative of the rotor position (θ_r) in state space form is expressed as:

$$p\theta_r = \omega_r \quad (19)$$

The potential of the neutral point with respect to the zero potential (v_{n0}) is required to be interpreted properly to avoid the imbalance in applied phase voltages.

This can be obtained by substituting (7) in (4) to (6) and adding them together to give

$$V_{a0} + V_{b0} + V_{c0} - 3V_{n0} = R(i_a + i_b + i_c) + (L_S + M)(pi_a + pi_b + pi_c) + (e_{an} + e_{bn} + e_{cn}) \quad (20)$$

Substituting (11) in (20) results in

$$V_{a0} + V_{b0} + V_{c0} - 3V_{n0} = (e_{an} + e_{bn} + e_{cn})$$
$$\Rightarrow V_{n0} = [V_{a0} + V_{b0} + V_{c0} - (e_{an} + e_{bn} + e_{cn})]/3 \quad (21)$$

The set of differential equations viz. (13),(14), (15), (18) and (19) defines the developed model in terms of the variables i_a, i_b, i_c, ω_r, and θ_r for the independent variable, time.

V. SIMULATION RESULTS

In this work the drive model with PI speed controller is developed and simulated in order to validate the model and the designed controller. For conducting the studies and analysis, this paper considers a typical industrial BLDC motor (Arrow Precision Motor Co., LTD) with importance specifications: 2hp, 1500rpm, 4 poles (Refer Appendix). Fig.5-12 shows simulated results.

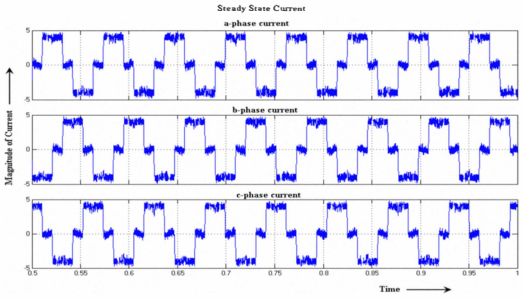

Figure 5. Stator phase currents

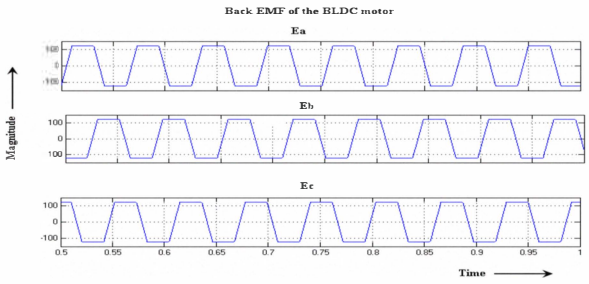

Figure 6. Trapezoidal back EMF

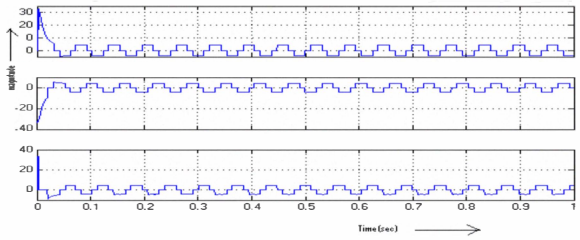

Figure 7. Reference current waveform

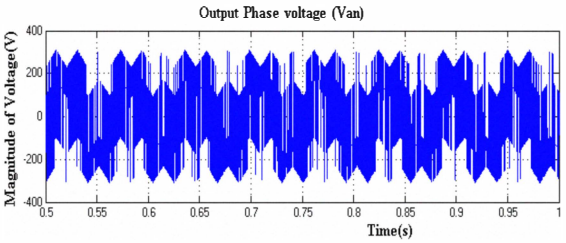

Figure 8. Representative phase voltage (van)

Fig.5 and Fig.6 show the stator phase currents and back emf respectively. Fig.7 shows the reference current. The typical phase voltage is diagrammed in Fig.8. Fig.9 shows the torque and the speed variations, and the motor speed quickly converges to the reference shortly after startup and recovers very well from the load torque disturbance as well as parameters variation. The moment of inertia value taken for this case is 0.013kg-m^2 and it reaches the steady state torque and speed suddenly at time 0.03seconds.When the moment of inertia is increased to 0.098kg-m^2 it takes 0.28 seconds to reach the steady state as evidenced in Fig.11. From the figure, it is inferred that increasing the moment of inertia will cause the settling time to increase.

Fig.10 and Fig.12 demonstrate the drive performance with step inertia change. The simulated results show that synchronization of the rotor speed is well done and the average electromagnetic torque is in equilibrium although the dynamic electromagnetic torque is not in equilibrium

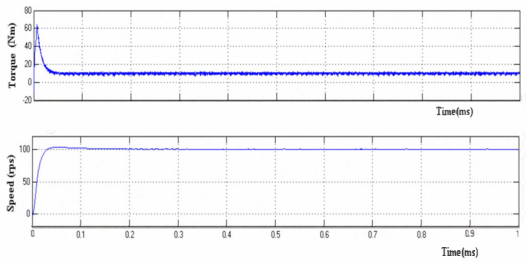

Figure 9. Torque and speed responses during startup transients

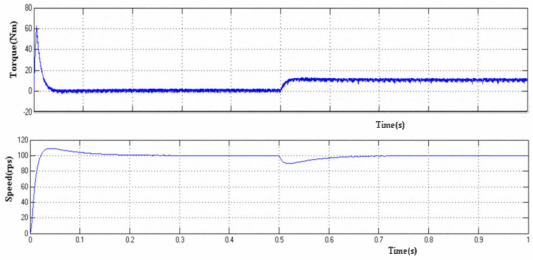

Figure 10. Torque and speed responses - step input change - moment of inertia 0.013 kg-m2 (step time 0.5 S)

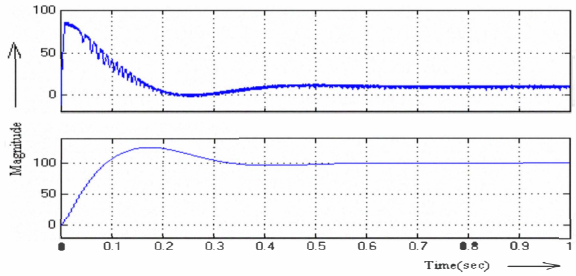

Figure 11. Torque and speed responses at moment of inertia 0.098 kg-m^2

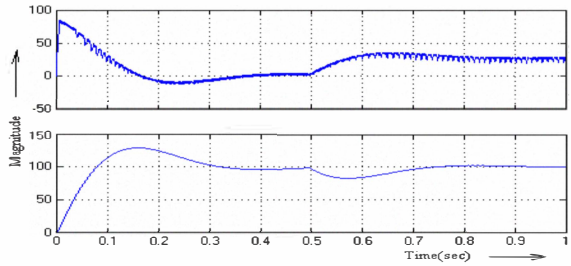

Figure 12. Torque and speed-Step input with moment of inertia 0.098 kg-m2 (step time 0.5 S)

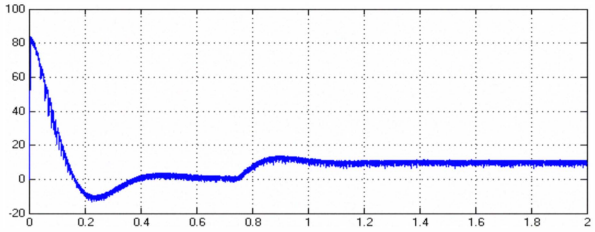

Figure 13. Step load torque (9Nm) at 0.75 step

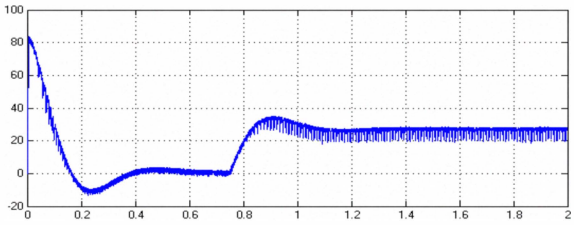

Figure 14. Step load torque (25 Nm) at 0.75

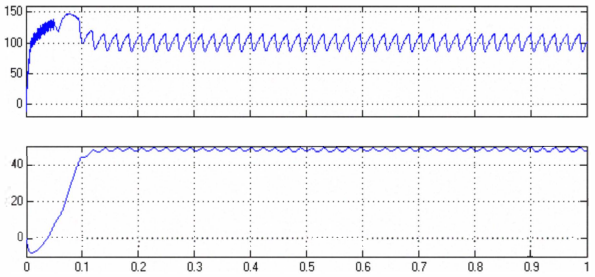

Figure 15. Application of heavy load (100 Nm)

Figures 13 to 16 show the performance while load changes. The results demonstrate that the designed PI controller is triumph in restoring the steady state. Fig.15 exhibits that iIf the load torque is increased into 100 Nm then the actual speed decreases into 48 RPS.

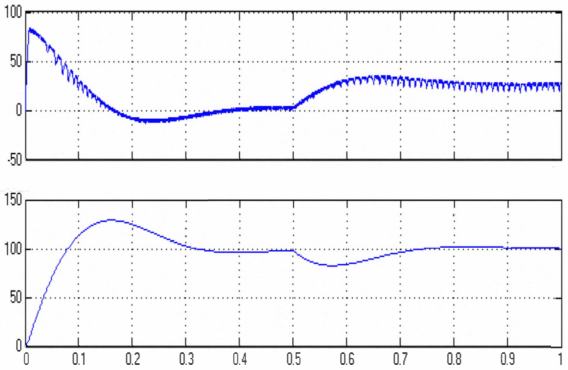

Figure 16. Load toque 25Nm at step of 0.5

VI. CONCLUSION

The nonlinear simulation model of the BLDC motors drive system with PI control based on MATLAB/Simulink platform is presented. The control structure has an inner current closed-loop and an outer-speed loop to govern the current. The speed controller regulates the rotor movement by varying the frequency of the pulse based on signal feedback from the Hall sensors. The performance of the developed PI algorithm based speed controller of the drive has revealed that the algorithm devises the behavior of the PMBLDC motor drive system work satisfactorily. Current is regulated within band by the hysteresis current regulator. And also by varying the moment of inertia observe that increase in moment of inertia it increases simulation time to reach the steady state value.

Consequently, the developed controller has robust speed characteristics against parameters and inertia variations. Therefore, it can be adapted speed control for high-performance BLDC motor.

REFERENCES

[1] Duane C.Hanselman, "Brushless Permanent-Magnet Motor Design", McGraw-Hill, Inc., New York, 1994.

[2] T.J.E.Miller, 'Brushless Permanent Magnet and Reluctance Motor Drives.' Oxford Science Publication, UK, 1989.

[3] R.Krishnan, Electric Motor Drives: Modeling, Analysis, and Control, Prentice-Hall, Upper Saddle River, NJ, 2001.

[4] P. Pillay and R. Krishnan, "Modeling, simulation, and analysis of permanent Magnet motor drives. Part II: The brushless dc motor drive," *IEEE Transactions on Industry Applications*, vol.IA-25, no.2, pp.274–279, Mar./Apr. 1989.

[5] R.Krishnan and A.J. Beutler, "Performance and design of an axial field permanent magnet synchronous motor servo drive," *Proceedings of IEEE IAS Annual Meeting*, pp.634-640,1985.

[6] In-Soung Jung,Ha-Gyeong Sung, Yon-Do Chun, and Jin-Hwan Borm, "Magnetization Modeling of a BondedMagnet for Performance Calculation of Inner- Rotor Type BLDC Motor", *IEEE Transactions on Magnetics*, vol.37, no.4, pp.2810-2813, July 2001.

[7] Qiang Han, Hee-Sang Ko, Juri Jatskevich, "Effect of Stator Resistance on Average-Value Modeling of BLDC Motor 120-Degree Inverter Systems", *Proceeding of International Conference on Electrical Machines and Systems* pp.481-486, Oct. 8-11, Seoul, Korea, 2007.

[8] Bhim singh, B P Singh and (Ms) K Jain," "Implementation of DSP Based "Digital Speed Controller for Permanent Magnet Brushless dc Motor" *Proceedings of IE(I) Journal-EL, 2002.*

[9] M.Lajoie-Mazenc, C.Villanueva, and J.Hector, "Study and implementation of a hysteresis controlled inverter on a permanent magnet synchronous machine," *IEEE Transactions on Industry Applications*, vol. IA-21, no.2, pp.408-413, March/April 1985.

[10] T.Sebastian and G.R.Slemon, "Transient Modeling and Performance of Variable Speed Permanent Magnet Motors." *IEEE Transactions on IA*, vol-25, no.1, pp.101, January/February 1989.

[11] A.Rubai and R.C.Yalamanchi, "Dynamic Study of an Electronically Brushless dc Machine via Computer Simulations." *IEEE Transactions on EC*, vol-7, no.1, pp.132, March 1992,

[12] P.C.K.Luk and C.K.Lee, "Efficient Modeling for a Brushless dc Motor Drive", *Conference Record of IEEE-IECON*, pp.188, 1994.

APPENDIX

Rating:	2.0 hp
Number of Poles:	4
Type of connection:	Star
Rated speed:	1500 rpm
Rated current:	4A
Resistance/phase:	2.8 Ω
Back EMF constant:	1.23V sec/rad
Inductance (L_s + M):	0.00521 H/phase
Moment of Inertia:	0.013 Kg-m^2/0.098 kg –m^2